REDUCTION OF OXYGEN ON $LaNiO_3$ IN ALKALINE SOLUTION

G. KARLSSON
Department of Chemical Technology, S-10044 Stockholm (Sweden)
(Received April 13, 1983)

Summary

Three different preparations of $LaNiO_3$ were examined on a rotating disc electrode, and gave comparable activities for high oxygen reduction in an alkaline solution. The activation energy for oxygen reduction is estimated to be 5 kcal/g mole. Heterogeneous reduction of the oxide to free $La(OH)_3$ and NiO takes place during prolonged exposure at low potentials, and is enhanced by a low temperature synthesis of the oxide. Fluoropolymer-bonded gas diffusion electrodes have a high activity but their lifetime is less than 24 h.

1. Introduction

Platinum, gold, and silver have long been used as oxygen electrocatalysts, but are expensive. Ideally, electrodes need not contain more than 5 - 10 g of noble metal/m^2, but even this could prohibit the use of air electrodes on a large scale. To a certain extent those obstacles can be overcome by recycling the noble metals.

Alkaline fuel cells with platinum on carbon–air cathodes are already being marketed commercially to utilize the hydrogen produced in chlorine–alkali and in chlorate plants [1]. The use of carbon is an alternative, for which long lifetimes have been reported but polarization is too high for some applications [2].

Metal oxides have been tried as electrocatalysts for oxygen reduction and several studies have been made of transition metal oxides with the perovskite structure. Cobalt based perovskites have been investigated extensively [3 - 6]. They are known to undergo reduction in the potential range where oxygen reduction takes place [7].

Matsumoto *et al.* [8] reported that the electrocatalytic activity of $LaNiO_3$ for oxygen reduction is comparable with that of platinum. They also showed that hydrophobic gas diffusion-electrodes, which give high currents, could be made [9].

0378-7753/83/$3.00

Instability problems, which seem to be caused by prolonged exposure to low potentials, are associated with perovskite based gas diffusion electrodes. The aim of this study was to investigate the reduction behaviour of $LaNiO_3$ and, in particular, oxygen reduction at higher temperatures to evaluate its potential as a fuel cell catalyst.

2. Experimental technique

2.1. Oxide preparation and analysis

The $LaNiO_3$ was prepared by various methods.

2.1.1. The acetate method

Lanthanum acetate and nickel acetate were dissolved in water and evaporated in a rotary evaporator at a temperature of 80 - 90 °C. The solid was decomposed in the flask at 280 - 320 °C and then ground in an agate mortar (used for all hand grinding) for 10 - 30 min. It was then slowly heated to the synthesis temperature (750 - 800 °C) and held there until the process was complete. Intermittent regrinding of the product at this stage accelerated the process, but to obtain pure $LaNiO_3$ six days were required to decompose the acetates. X-ray diffraction showed that the unreacted oxides only decreased gradually as the active oxygen increased. Ultimately, however, it could be dissolved in 6M HCl without any residue. The active oxygen corresponded to the formula $LaNiO_{2.96}$ with cubic structure.

X-ray diffractometry shows that the evaporation of the acetate solution gave a mixture which was so crystalline neither the dispersion nor the mixing of the lanthanum and nickel was good. After the decomposition the X-ray diffraction peaks were very broad indicating small crystallites. The mixing of the elements, however, was probably not much better than it was before, because no true melt was formed during decomposition. The decomposed acetates were slightly reducing towards iodine in hydrochloric acid.

2.1.2. The nitrate method

The hydrated nitrates of lanthanum and nickel were melted together in their water of crystallization which was evaporated by slowly increasing the temperature to 200 °C. The water-free nitrates were ground by hand for one minute, partially decomposed at 450 °C for one hour, and reground for a further 5 min. Thereafter they were heated to 750 °C in air for 24 h when X-ray diffraction showed that the perovskite formation was complete.

2.1.3. The hydroxide method

0.15 - 0.20 molar solutions of the nitrates of nickel and lanthanum were added slowly to a 5 - 6 fold excess of 1 molar, KOH at 60 °C. To obtain good mixing the nitrate solution was added through a fine capillary tubing onto the shaft of a stirrer rotating at 1800 rpm. The precipitate was washed with distilled water by repeated decantations until incipient peptization

became apparent. It was then vacuum filtered on a Büchner funnel washed with two to three volumes of distilled water, dried, and reground. Some batches, however, were washed with methanol which prevented shrinkage of the filter cake during drying and made regrinding unnecessary. The dried precipitate was transferred to a small porcelain crucible and kept at 700 °C for 18 h in pure oxygen.

2.1.4. Miscellaneous methods

Different methods were tried using Li_2CO_3, K_2CO_3, Na_2CO_3 and $NaLiCO_3$ fluxes with La_2O_3, Ni, "Ni_2O_3" (KEBO-GRAVE), and $NiCO_3$ for the lanthanum and nickel. Higher synthesis temperatures (800 - 900 °C) and more regrinding were needed than for the other methods to obtain pure $LaNiO_3$.

2.1.5. Analytical methods

The oxide preparations were analyzed by X-ray diffractometry and chemical analysis. The latter consisted of dissolving 0.2 - 0.4 g of the oxide in 50 - 70 ml of, 6 molar HCl with 0.5 g of KI and titrating the liberated iodine with standard 0.1 molar $Na_2S_2O_3$. This enabled the amount of "active oxygen", *i.e.*, the amount of trivalent nickel to be determined. The unreacted NiO remained undissolved.

2.2. Electrode preparation

2.2.1. Electrodes for rotating disc experiments

Three electrode discs were used. The first was made from $LaNiO_3$ with 12% of the nickel present as unreacted NiO. This powder was compressed into a steel mould to form a pellet which was sintered in air at 1050 °C for 2 h. After cooling slowly it was impregnated with Halocarbon® wax at 180 °C under vacuum to eliminate porosity. The final step was repeated several times to ensure penetration.

The second electrode was made with pure $LaNiO_3$ produced by the acetate method and kept at 750 - 800 °C for six days. The oxide was mixed with 13 wt.%, TFE-powder, Hostaflon® pressed in the steel mould, and impregnated with Halocarbon wax®.

The third electrode disc was made in the same way as the second but using oxide made by the nitrate method.

Before each experiment the disc electrodes were polished with emery paper and rinsed in hot KOH solution.

2.2.2. Electrode for discharge experiments

This was made in the same way as the second electrode disc, except that the impregnation was omitted.

2.2.3. Gas diffusion electrode

Two gas diffusion electrodes were made of high surface area (9 m^2/g) $LaNiO_3$, produced by the hydroxide method. (The specific surface area was

measured by the BET-method using krypton as adsorbate.) The oxide was thoroughly mixed with Teflon®-FEP dispersion, in the proportion 2:1 by weight, together with some water. This mass was dried, sieved, and washed with methanol. It was dried again, sieved onto nickel screens which had 2 nickel wires spot welded to them, and pressed at 100 MPa. Finally, the electrodes were cured at 260 °C for 30 min. They were then put into acrylic half cells and supplied with pure oxygen at atmospheric pressure with no differential pressure. The loadings of the two electrodes were 32 mg and 45 mg per square centimeter.

The HgO/Hg reference electrodes had fine PTFE tubes which served as Luggin capillaries and kept the *IR*-drop below 5 mV.

2.3. Rotating disc electrode experiments

The cell used in these experiments had three compartments, one of 500 ml volume for the rotating working electrode and two smaller compartments for the reference electrode and for the counter electrode. The hydrogen reference electrode was a small piece of nickel gauze with PTFE-bonded platinum black and its chamber linked to the center of the main compartment with a glass capillary. The counter electrode was a piece of nickel wire. Glass frits were inserted in the connections between the main compartment and the others. The main compartment was equipped with two porous glass frit bubblers. Gases entering the cell were passed through wash bottles filled with the same electrolyte as the cell and kept at the same temperature. The nitrogen used was passed through acidified chromous chloride. Potential were controlled with a Wenking potentiostat. The rotating electrode was driven by a tachogenerator controlled d.c. motor *via* a flexible cable and steel shaft. The electric contact was made through a silver filled carbon brush which contacted a gold plated part of the steel shaft. The steel shaft was hot-pressed into a 9 mm dia. Kel-F® cylinder with an external screw thread for mounting exchangeable electrode tips. The electrode disks were hot-pressed into these tips which were of the same diameter as the Kel-Fe® cylinder.

2.4. Control of electrolyte purity

An estimate of electrolyte purity can be obtained from potential cycling of the platinum electrode. It is a common practice to cycle platinum repeatedly between oxygen evolution and hydrogen evolution to purify the electrolyte and to ensure reproducible results [10]. Oxygen evolution cleans by oxidizing (desorbing) the adsorbed organic molecules and cathodic hydrogen evolution prevents the oxide layer on the platinum from becoming too thick and refractory. After 3 or 4 cycles the currents measured at constant potential become reproducible. During the cathodic part of the cycle, however, the current decreases smoothly at a rate which is enhanced at higher rotation speeds. At above 1000 rpm the current, at constant potential, decreases linearly with time, as shown in Fig. 1. The time taken to halve the current ($t_{1/2}$), when the electrode was rotated at 6000 rpm, was used as the indicator of electrolyte purity.

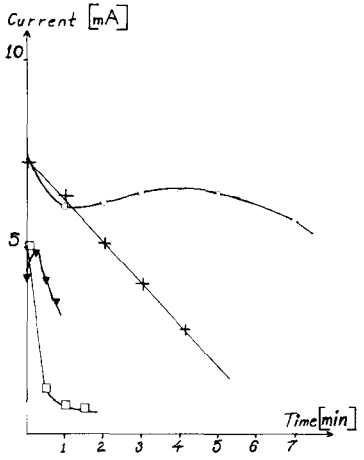

Fig. 1. Time dependency of hydrogen evolution on platinum in 5 molar KOH. Constant potential −0.1 *vs.* H_2. After 5 activation cycles (2 min at 2.1 V and 2 min at −0.1 V). ▼, Rubber contaminated electrolyte; □, rubber contaminated electrolyte with rotation; ○, electrolyte made from single distilled water; +, as previously with rotation.

2.5. Monitoring the discharge products and discharge potential

For this experiment the pores of the electrode disc were not wax-impregnated and the whole electrode could, therefore, be discharged. It was squeezed, in a small, sealed glass-cell, with the oxygen expelled by nitrogen, between two gold-plated foils. One foil was the current lead and the other was used for potential measuring. After discharge each electrode was washed, dried, crushed, sieved, and analysed by X-ray diffractometry.

3. Results

3.1. Purity of electrolyte

To monitor the purity of the electrolyte, experiments were run with platinum electrodes; the kinetics of oxygen reduction on platinum in alkaline solutions are well known. The initial experiments, using a rotating electrode from Beckman, demonstrated the importance of isolating the mechanical parts from the electrolyte to prevent contamination by grease. A nitrile rubber 'O-ring' seal was tried but had to be abandoned because it contaminated the electrolyte even after being leached in hot KOH solution for one day before installation. In subsequent assemblies the sealing was accomplished by using a very narrow slit filled with Halocarbon®-grease.

Different methods of purification were then tested. The electrolyte was treated with high surface area absorbents such as platinum black, active carbon, thoroughly leached Raney nickel and high surface area $La_{0.5}Sr_{0.5}Co_3$. One gram per litre of the platinum black was used and 10 g/l of the other absorbents. Neither the active carbon nor the perovskite were found to give

significant improvement, as indicated by a measure of $t_{1/2}$ (see Section 2.4). With platinum black and Raney nickel, however, $t_{1/2}$ (increased from 200 s to over 1000 s. When double distilled water was used to make the electrolyte, $t_{1/2}$ increased to 300 s.

Measurements of the Tafel slope and the open circuit potential showed that the oxygen reduction characteristics were not influenced much by these different treatments. For the non-purified electrolytes the open-circuit potential was around +980 mV *vs.* reference hydrogen electrode, for the platinum and Raney nickel treated electrolytes, and with the electrolyte made from double distilled water it was nearly 1020 mV *vs.* reference hydrogen electrode. The oxygen reduction kinetics agreed quite well with earlier reports [11 - 13]. An exchange current density of 3 - 6 × 10^{-10} A/cm^2 and a Tafel-slope of 0.055 - 0.060 V/decade were recorded, whereas the non-purified electrolytes gave a Tafel slope close to 70 mV/decade.

The sealing of the cell was proved to be effective; when cleaned and filled with pure electrolyte the same oxygen reduction curves could be recorded for several days.

It was concluded that the purity of electrolyte made using double distilled water would be good enough for the $LaNiO_3$ experiments.

3.2. Cathodic behaviour of $LaNiO_3$

The first rotating disc experiment with $LaNiO_3$ gave the cathodic current plotted in the Tafel diagram of Fig. 2. The behaviour at room temperature agrees quite well with what has been reported by Matsumoto *et al.* [8, 9]. The Tafel slope is close to 50 mV/decade. Below 0.92 V the Tafel slope increases but this was not investigated in detail because it was suspected to be connected with irreversible reduction of the oxide. The current density at this potential is well below the limiting current density, which is several mA per square centimeter.

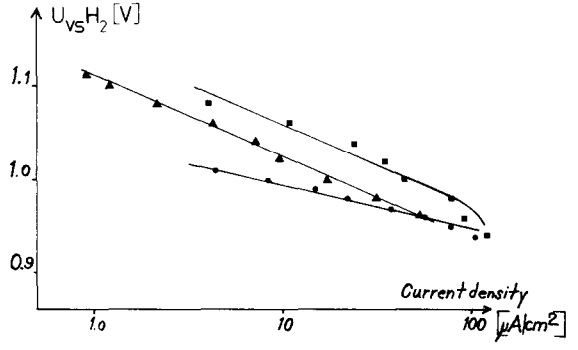

Fig. 2. Polarisation curve of $LaNiO_3$ disc electrode in oxygen saturated 1 molar KOH. Speed of rotation 6000 rpm. ■, 77 °C; ▲, 55 °C; ●, 22 °C. Sintered electrode containing some NiO.

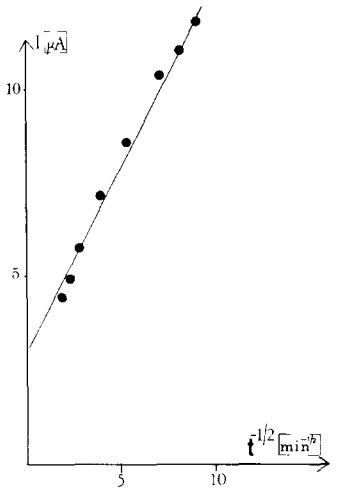

Fig. 3. Plot of current *vs.* square root of inverted time for a potentiostatic step. Electrode $LaNiO_3$ equilibrated at 1 V for 5 h then the potential was changed to 0.9 V. Nitrogen purged electrolyte.

The polarization curve was recorded by increasing or decreasing the potential in 10 mV or 20 mV steps. At room temperature the current stabilized within 10 - 20 min and after 30 min the polarization curve was the same in cathodic and anodic directions.

At the higher temperatures the currents did not stabilize completely, even after 3 days.

To test the speed with which an electrode disc reacts to changes in potential it was stabilized for 5 h at 1.0 V in a nitrogen saturated electrolyte, then the potential was changed to 0.9 V. Within an hour the current had decreased to 4 μA. Plotting the current against the inverted square root, as in Fig. 3, gives quite a good linear fit, especially as the electrode disc is neither completely dense nor completely homogeneous. The slope could be partly accounted for by some of the current being controlled by diffusion through a depleted layer. This current is so small, however, that control by the diffusion of water is not probable. It is more likely to be connected with the homogeneous reduction of the oxide, where diffusion takes place in a solid phase. There is also a residual current of 3 μA, which might come from heterogeneous breakdown of the oxide.

3.3. Time stability of oxygen reduction

For this experiment the second electrode disc was used. The cathodic behaviour, in oxygen saturated electrolyte, of this electrode at room temperature was found to be different from the first $LaNiO_3$ electrode, as shown in Fig. 4. The currents at potentials above 0.92 V were much higher and the Tafel-slope was greater than for the first electrode. The response of the electrode to changes in potential was fast. The polarization curve was recorded with increasing potentials.

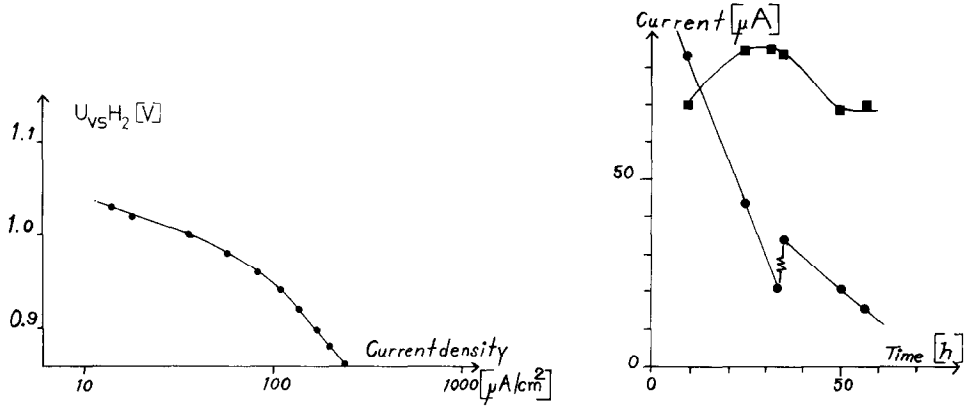

Fig. 4. Polarisation curve of $LaNiO_3$ in oxygen saturated 1 molar KOH, 22 °C. Electrode cold-pressed from pure $LaNiO_3$. Electrode rotated at 6000 rpm.

Fig. 5. Oxygen and oxide reduction for $LaNiO_3$, in 1 molar KOH at 55 °C. ■, oxide reduction; ●, oxygen reduction. Same electrode as in Fig. 4.

To examine its potential as a fuel-cell electrocatalyst the temperature was increased to 55 °C with the potential kept at 0.91 V. The electrolyte was occasionally purged with nitrogen and the current was measured. The oxygen reduction current was found to differ depending on whether it was under oxygen or under nitrogen atmosphere, see Fig. 5. The activity for oxygen reaction reduced rapidly while that for oxide reduction did not change much. This stability of the oxide reduction clearly indicates that it is mainly heterogeneous. After 35 h the electrode was polished to remove the reduced layer and, although the oxygen reduction current increased, it was still far from its original value. The ohmic resistance of the electrode disc had also increased by a factor of 40, indicating the poor conductive properties of the reduced layer.

3.4. Temperature effects on oxygen reduction

The third electrode disc was used in this experiment in which the oxygen reduction was measured as the difference between the currents under nitrogen and under oxygen.

This electrode took longer to stabilize but seemed to be more reactive than the one used in the first experiment. There may, however, be a difference in the exposed active area and it is possible that the wax used in impregnation had not penetrated all the pores in the more finely grained oxide. Only a few points were recorded because of the long stabilization times (around 1 h for each change): these are presented in Table 1. A change in temperature from 0 °C to 22 °C caused the current to double, corresponding to an activation energy of approximately 5 kcal/mole which agrees quite well with the value reported by Hibbert and Tseung [14] for NiO above its Néel temperature.

TABLE 1

Temperature dependence of oxygen reaction
Current density $\mu A/cm^2$

Potential *vs.* H_2 (V)	Temperature (°C)	
	0	22
0.92	100	210
0.90	—	330
0.88	185	390

3.5. Gas diffusion electrodes

The polarization curves for the gas diffusion electrodes, shown in Fig. 6, were measured 16 h after the electrodes were submerged in the electrolyte. At current densities higher than 5 mA/cm^2 the curves are linear, with slopes (equal to the "pseudo" surface resistivity) which are high (2 - 3 Ω cm^2) compared with other gas diffusion electrodes [7]. Most gas diffusion electrodes have "pseudo" surface resistivities lower than 1 Ω cm^2 when used with pure oxygen.

The performance of the electrode is not stable, as is seen in Fig. 7. This is not likely to be caused by wetting, as the manufacturing procedure gives a good result when making carbon electrodes. In these the fluoropolymer content is high, around 40% by volume and long times were allowed for the electrode to become stably wetted before being used. The electrodes gave less current when applying a slight differential pressure.

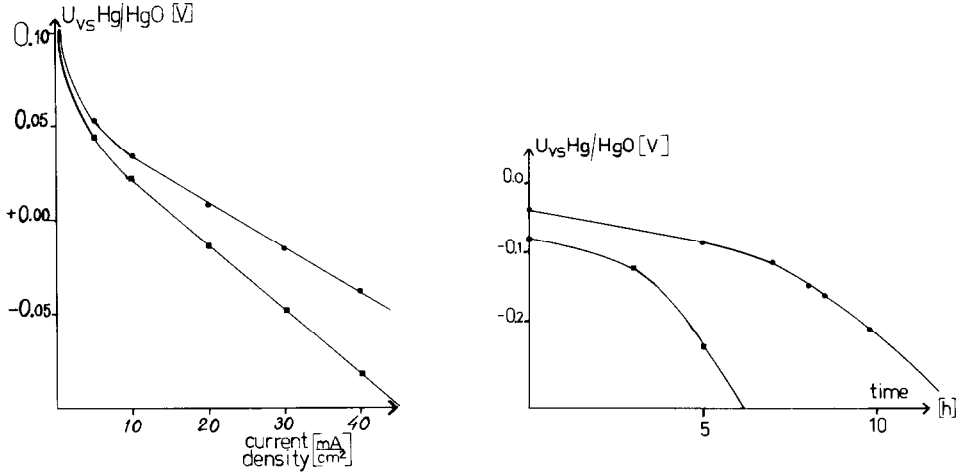

Fig. 6. Polarization curve for FEP-bonded $LaNiO_3$ gas-diffusion electrodes using pure oxygen in 5 molar KOH. Loadings: ●, 45 mg/cm^2; ■, 32 mg/cm^2. The measured potentials are without external electrolyte *IR*-drop.

Fig. 7. Variation of potential with time at a current density of 40 mA/cm^2 for the electrodes in Fig. 6.

3.6. Discharge products and potentials

Three experiments were performed. Two at 55 °C with discharge levels corresponding to $\delta = 0.2$ and $\delta = 0.14$ if the compound is written $LaNiO_{3-\delta}$ and one at 22 °C when the discharge level corresponded to $\delta = 0.11$. The discharge potentials are given in Figs. 8 and 9, and the X-ray diffractograms in Fig. 10(a) - (c).

At 55 °C heterogeneous reduction takes place at high potential, above that where oxygen reduction is useful. The discharge potential in Fig. 8 is given for the experiment with the high discharge level ($\delta = 0.2$). The discharge curve for the low discharge level ($\delta = 0.14$) is similar to that of Fig. 8. At both discharge levels $La(OH)_3$ and $Ni(OH)_2$ are found in the X-ray diffractograms, see Fig. 10(a) and (b).

The low discharge experiment was interrupted at a potential of +0.1 V *vs.* Hg/HgO. An anomaly is that the $Ni(OH)_2$ diffraction peak at a diffraction angle of 38.6° is stronger in the less discharged sample. One day after discharge there was no sharp peak at 38.6° but a month later both samples had sharp peaks at this value. The $La(OH)_3$ peaks at 27.5°, 27.9°, 39.5° and 48.5° were not affected by storage.

At 22 °C the discharge takes place at lower potentials, about the same as, or below, those useful for oxygen reduction. The runs were terminated when the potential fell to 0.3 V *vs.* Hg/HgO because such low potentials are not useful in metal–air batteries. The diffraction peaks of $La(OH)_3$ are weaker and not so sharp compared with the samples discharged at 55 °C, see Fig. 8(c). The main difference is that a diffraction peak of NiO is found at 37.4° and the diffraction peak of $Ni(OH)_2$ at 38.6° is missing.

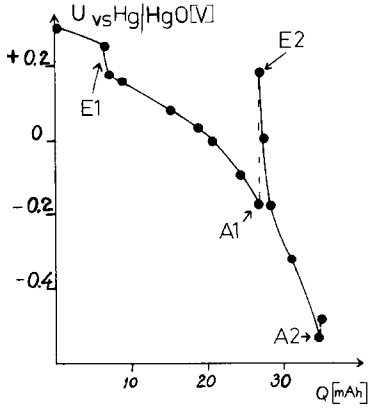

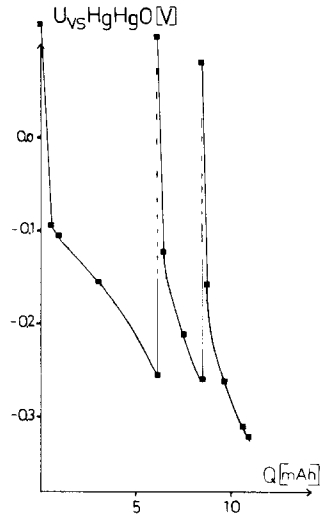

Fig. 8. Discharge of $LaNiO_3$ in 1 molar KOH. Current density 0.3 mA/g after E1 0.9 mA/g. Discharge interrupted at A1 for 2 h, continued at E2 and stopped at A2. t = 55 °C.

Fig. 9. Discharge of $LaNiO_3$ in 1 molar KOH at 22 °C. Current density 0.3 mA/g. Discharge twice interrupted overnight.

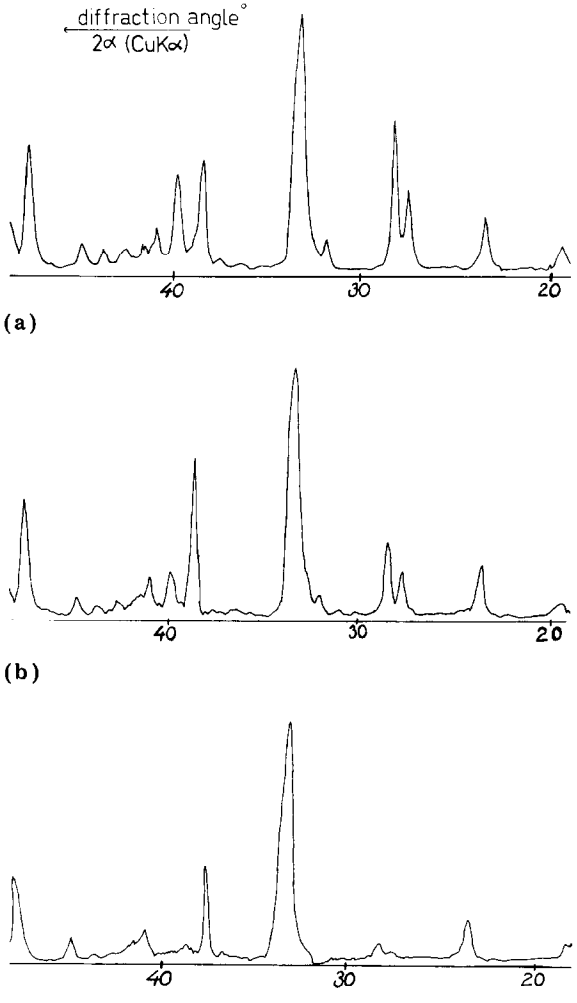

Fig. 10. X-ray-diffractograms. (a) Discharged to $LaNiO_{2.80}$ at 55 °C; (b) discharged to $LaNiO_{2.86}$ at 55 °C; (c) discharged to $LaNiO_{2.89}$ at 22 °C.

4. Discussion

The experiments showed that $LaNiO_3$ is thermodynamically and kinetically unstable when made cathodic *vs.* the reversible oxygen electrode. At the start of reduction there was an homogeneous phase when the outer parts of the oxide grains lost oxide ions or were hydroxylated according to either

$$LaNiO_3 + \delta H_2O + 2\delta e^- \longrightarrow LaNiO_3 + 2\delta OH^-$$

or

$$LaNiO_3 + \delta H_2O + \delta e^- \longrightarrow LaNiO_3H_\delta + \delta OH^-$$

The increased fraction of Ni(II) in the oxide causes it to become less stable because of the large difference in ionic radius between Ni(III) and Ni(II). Matsumoto *et al.* [15] showed that a wet proofed $LaNiO_3$ disc electrode held at −0.8 V *vs.* Hg/HgO for 10 h did change its properties. The X-ray diffraction peaks become ambiguous and the resistance increased significantly.

It has been shown that, at 55 °C, the reduction current at constant potential is stable and $La(OH)_3$ and $Ni(OH)_2$ are produced, indicating that reduction is heterogeneous, as illustrated by the reaction:

$$LaNiO_3 + 3H_2O + e^- \longrightarrow La(OH)_3 + Ni(OH)_2 + OH^-$$

It is not easy to see how to avoid this difficulty.

The reduction of MnO_2 takes place in two stages, first homogeneously in the solid phase and later heterogeneously [16]. MnO_2 exists in several allotropic forms and their reduction potentials differ by almost 0.2 V.

$LaNiO_3$ exists in mainly two allotropic forms, "hexagonal" and "cubic". When the oxide is synthesized below 800 °C without using fluxes the cubic form is formed. At higher temperatures and when using fluxes the hexagonal variety of the oxide is formed.

Obayashi and Kudo [17] have shown that the hexagonal form (with a rhombohedral distortion) is converted to the cubic form at 940 °C. It is not clear whether this means that the hexagonal form is the thermodynamically stable form at low temperatures or not. The transformation at 940 °C might have taken place for kinetic reasons. Matsumoto *et al.* kept a sample of cubic $LaNiO_3$ at 850 °C for 2 days without transformation suggesting that it is the cubic form which is stable at low temperatures. The synthesis conditions for hexagonal $LaNiO_3$ give preparations with low surface areas which are less useful for practical electrodes.

It is also known that the heterogeneous reduction of MnO_2 can be reduced by using dilute electrolyte, 1 molar or less; the solubility of Mn(III) decreases with the concentration of the caustic solution. This is not practical for fuel cells and metal–air batteries because a strong electrolyte is needed for conductivity reasons.

La_2O_3 is hygroscopic: dense samples are converted completely into $La(OH)_3$ by humid air at room temperature in less than 50 h [18]. This could be one of the reasons for the instability of $LaNiO_3$. Nd_2O_3 hydroxylates at a lower rate than La_2O_3 [18] and Kudo *et al.* [7] substituted Nd for La in $La_{0.8}Sr_{0.2}CoO_3$ and achieved good stabilisation. Only a minor part of La, however, can be substituted with Nd in $LaNiO_3$ according to Wold *et al.* [19] and Matsumoto *et al.* [9].

Acknowledgement

This study was financially supported by Carl Tryggers Stiftelse and the Swedish National Board for Technical Development.

References

1 *Oxy-hydrogen–Air Fuel Cell*, Pamphlet from Occidental Research Corp. Available from A. I. Emery, Program Director, Fuel Cell Project. 2100 S E. Main Street Irvine, CA. 92714, USA.
2 G. Duperray, G. Marcellin and B. Pichon, in J. Thompson (ed.), *Power Sources 8*, Academic Press, London, New York, 1981, p. 489.
3 T. Kudo, H. Obayashi and M. Yoshida, *J. Electrochem. Soc., 124* (1977) 321 - 325.
4 A. C. C. Tseung and H. L. Bevan, *J. Electroanal. Chem., 45* (1973) 429 - 438.
5 T. Kudo, H. Obayashi and T. Geijo, *J. Electrochem. Soc., 122* (1975) 159 - 163.
6 F. R. van Buren, G. H. J. Broers, A. J. Bouman and C. Boesveld, *J. Electroanal. Chem., 88* (1978) 353 - 361.
7 H. Obayashi and T. Kudo, *Denki Kagaku, 44* (1976) 503 - 507.
8 Y. Matsumoto, H. Yoneyama and H. Tamura, *Chem. Lett.*, (1975) 661 - 882.
9 Y. Matsumoto, H. Yoneyama and H. Tamura, *J. Electroanal. Chem., 83* (1977) 167 - 176.
10 S. D. James, *J. Electrochem. Soc., 114* (1967) 1113 - 1119.
11 W. M. Vogel and J. T. Lundquist, *J. Electrochem. Soc., 117* (1970) 1512 - 1516.
12 D. B. Sepa, M. V. Vojnovic and A. Damjanovic, *Electrokhimiya, 25* (1980) 1491 - 1496.
13 A. Damjanovic, M. A. Genshaw and J. O. M. Bockris, *J. Electrochem. Soc., 114* (1967) 1107 - 1112.
14 D. B. Hibbert and A. C. C. Tseung, *J. Electrochem. Soc., 125* (1978) 74 - 78.
15 Y. Matsumoto, H. Yoneyama and H. Tamura, *J. Electroanal. Chem., 80* (1977) 115 - 121.
16 A. Kozawa, Electrochemistry of manganese dioxide, in K. V. Kordesh (ed.), *Batteries*, Vol. 1, Dekker, New York, 1974, pp. 385 - 519.
17 H. Obayshi and T. Kudo, *Jpn. J. Appl. Phys., 14* (1975) 330 - 335.
18 M. Foex, *Bull. Soc. Chim. Fr.*, (1961) 109 - 117.
19 A. Wold, B. Post and E. Banks, *J. Am. Chem. Soc., 79* (1957) 4911.